International Journal of Wavelets, Multiresolution
and Information Processing
Vol. 6, No. 6 (2008) 895–906

SUBBAND VARIANCE COMPUTATION OF HOMOSCEDASTIC ADDITIVE NOISE IN DISCRETE DYADIC WAVELET TRANSFORM

ARIANNA MENCATTINI* and MARCELLO SALMERI†

Department of Electronic Engineering
University of Rome "Tor Vergata"
Via del Politecnico 1, 00133 Rome, Italy
**mencattini@ing.uniroma2.it*
†salmeri@ing.uniroma2.it

FEDERICA CASELLI

Department of Civil Engineering
University of Rome "Tor Vergata"
Via del Politecnico 1, 00133 Rome, Italy
caselli@ing.uniroma2.it

BERARDINO SCIUNZI

Department of Mathematics, University of Calabria
Via Pietro Bucci, 87036 Arcavacata di Rende (CS), Italy
sciunzi@mat.unical.it

ROBERTO LOJACONO

Department of Electronic Engineering
University of Rome "Tor Vergata"
Via del Politecnico 1, 00133 Rome, Italy
lojacono@ing.uniroma2.it

Received 18 January 2008
Revised 16 June 2008

The paper deals with noise power variation that occurs when Discrete Dyadic Wavelet Transform (DDWT) is applied to signals affected by Wide Sense Stationary (WSS) additive white noise owing to the use of a non orthonormal expansion. An exact relationship between the noise variance in the original signal and the noise variance in the wavelet coefficients at a generic level is derived. This relationship is crucial in the application of wavelet thresholding for signal denoising to properly select the threshold in each subband.

Keywords: Discrete Dyadic Wavelet Transform; homoscedastic additive noise; subband noise variance.

AMS Subject Classification: 42C40, 60H40

1. Introduction

Discrete Dyadic Wavelet Transform (DDWT) represents a powerful tool in signal analysis and processing.[10] It belongs to the class of redundant frame expansions of signals which exhibits translation invariance (overcoming orthogonal wavelet transforms) and very good multiresolution analysis capabilities, at the expense of undecimation. In recent years, DDWT has been extensively used in various fields[11,16] and specially in medical image processing.[4,9,14,17]

In most applications, noise reduction is a central issue and a lot of wavelet-based denoising algorithms may be found in the literature.[18,19] Most of them are based on *Wavelet Thresholding*, a simple and effective technique introduced in a seminal work by Donoho and Johnstone.[3] The basic principle of wavelet thresholding is to identify and zero out, at each level of wavelet decomposition, those coefficients which are under a certain level-dependent threshold. The motivation behind this approach is that, due to the sparsity of wavelet representation, small coefficients are likely to contain mostly noise while large coefficients are related to important signal features. The key aspect of this strategy is to optimally choose the thresholds: too high thresholds turn out in loss of information, too low thresholds cause a remaining noise (which may be dramatically emphasized in a further signal-enhancement step). In almost all threshold-selection methods, the thresholds are function of noise power.[1–3,8] However, when using DDWT noise power does not remain constant through the decomposition levels[5] and has to be determined at each level to set the proper subband threshold. A possible approach is to estimate the noise variance of wavelet coefficients in each subband, but this is a complex and time-consuming task.

In this paper, we provide the relation between noise variance in the original signal and noise variance in each subband of the DDWT decomposition, under the assumption of a WSS additive white noise in the original signal. In this way, only noise variance in the original signal has to be estimated. We address both the one-dimensional and the two-dimensional case. The proof of the main results will be accomplished by using complex analysis and random process theory.

The paper is organized as follows. In Sec. 2, we recall main properties of DDWT and its fast implementation. In Sec. 3, we provide the expressions of noise variance in each subband; the proofs of these expressions are given in Secs. 4 and 5, for one-dimensional and two-dimensional cases, respectively. Finally, Sec. 6 is devoted to conclusions and remarks.

2. Discrete Dyadic Wavelet Transform

In this paper, we consider the DDWT firstly introduced by Mallat,[10,11] which represents a translation invariant and redundant representation. We recall only the fundamental properties of DDWT, referring the reader to Refs. 9 and 10 for an exhaustive description. We consider the particular subclass of DDWT based on the so called *Spline Dyadic Wavelets* since the scaling function $\phi(x)$ is a box spline

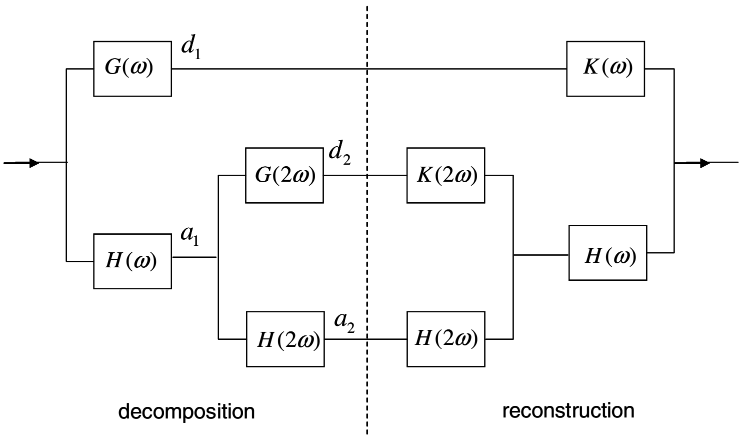

Fig. 1. Filter bank implementation of DDWT in one-dimensional case ($D = 2$).

function whose Fourier transform is given by $\Phi(\omega) = (\sin(\omega/2)/(\omega/2))^{z+1}e^{(-\iota\varepsilon\omega/2)}$ (where $\varepsilon = 1$ if z is even and zero otherwise). The scaling function ϕ, the wavelet ψ and the dual frame $\tilde{\phi}$, $\tilde{\psi}$ are designed with filters $h(n)$, $g(n)$, $\tilde{h}(n)$, and $\tilde{g}(n)$ with Fourier transform given by

$$H(\omega) = e^{\iota\omega s_1}\cos^{p+1}\left(\frac{\omega}{2}\right), \quad G(\omega) = e^{\iota\omega s_2}\left(2\iota\sin\left(\frac{\omega}{2}\right)\right)^r, \tag{2.1}$$

where $p \in \mathbb{N}$, $s_1 = \frac{1}{2}((p+1)\mathrm{mod}\,2)$, $r \in \{1,2\}$, $s_2 = \frac{1}{2}(r \bmod 2)$, $\tilde{H}(\omega) = H(\omega)$, and $\tilde{G}(\omega) = K(\omega)$ with $K(\omega) = (1 - |H(\omega)|^2)/G(\omega)$. A fast dyadic wavelet transform (and its inverse) may be evaluated by a filter bank algorithm, called *algorithme à trous*.[7] Let D be the number of decomposition levels. The filter bank for one-dimensional case is shown in Fig. 1, where d_m and a_m denote detail and approximation coefficients at decomposition level m respectively, $m = 1,\ldots,D$ (two decomposition levels are considered in the picture). Figure 2 shows the two-dimensional filter bank (again for $D = 2$). Let us observe that in this case we have vertical ($d_{v,m}$) and horizontal ($d_{h,m}$) detail coefficients. Filters H, G and K are the same as in the one-dimensional case, while filter $L(\omega)$ is obtained by $L(\omega) = (1 + |H(\omega)|^2)/2$. In the figure, the notations ω_v and ω_h mean that the corresponding filter is applied to the rows and to the column of the input signal respectively. This paper deals, in particular, with the cases $p = 1$, $r = 1$ and $p = 1$, $r = 2$.

3. Subband Noise Variance Computation

In this section, we provide a direct relation between noise variance in original signal (which may be estimated by several methods[6,12,15]) and noise variance at each level m, $m = 1,\ldots,D$. Let us start with the one-dimensional case and consider again the block diagram in Fig. 1, with particular attention to decomposition levels.

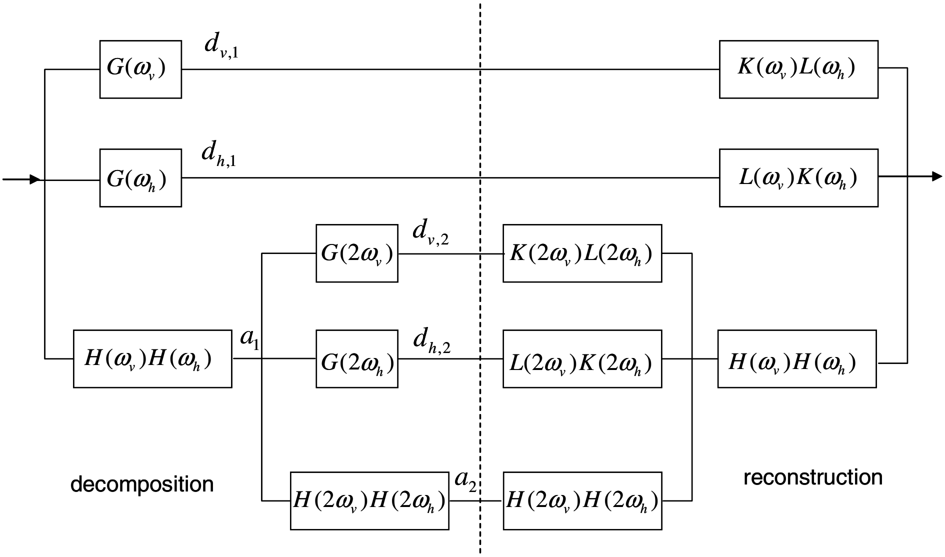

Fig. 2. Filter bank implementation of DDWT in two-dimensional case ($D = 2$).

Suppose now that the input signal is affected by a Wide Sense Stationary (WSS) additive white noise $x(n)$ with variance σ_x^2 and autocorrelation $R_{x\,x}(n) = \delta(n)\,\sigma_x^2$, where $\delta(n)$ is the *unit sample sequence*. We will derive the relation between σ_x^2 and $\sigma_d^2(m)$, and the relation between σ_x^2 and $\sigma_a^2(m)$ for each level $m = 1, \ldots, D$, where $\sigma_d^2(m)$ and $\sigma_a^2(m)$ are the noise variance in the sequence $d_m(n)$ and $a_m(n)$, respectively. In this paper, we only address a homoscedastic additive random noise, since we suppose that σ_x^2 is constant along signal. The case of heteroscedastic additive random noise is under investigation, with particular attention to the case of a signal dependent additive random noise (e.g., Poisson noise) often encountered in Charged Coupled Device (CCD) acquisition systems or in scan film radiography.[13]

We recall some basic notions about stationary random process and linear systems. Suppose that a random processes $x(n)$ is a WSS white noise and it is the input to a linear digital system characterized by an impulse response $f(n)$. Let us denote with $y(n)$ the output of the system. Then the power spectrums of $y(n)$ and $x(n)$, $S_{yy}(\omega)$ and $S_{xx}(\omega)$, respectively, satisfy $S_{yy}(\omega) = S_{xx}(\omega)|F(\omega)|^2$, where $F(\omega)$ is the Fourier transform of the impulse response $f(n)$ (i.e. the transfer function of the filter). Then, the autocorrelation of process $y(n)$ is given by

$$R_{yy}(n) = \frac{1}{2\pi}\int_{-\pi}^{\pi} S_{yy}(\omega)e^{\iota\omega n}d\omega = \frac{1}{2\pi}\int_{-\pi}^{\pi} S_{xx}(\omega)|F(\omega)|^2 e^{\iota\omega n}d\omega.$$

Recall that for any linear system with input $x(n)$, output $y(n)$ and impulse response $f(n)$, it holds $E[y(n)] = E[x(n)] * f(n)$, where E denotes the mean value and $*$ is the convolution operator. Thus, if $x(n)$ is a WSS white random process, then $y(n)$

is zero mean. Therefore $\sigma_y^2 = R_{yy}(0)$ and hence

$$\sigma_y^2 = \frac{1}{2\pi}\int_{-\pi}^{\pi} S_{xx}(\omega)|F(\omega)|^2 d\omega.$$

Finally, since we have $S_{xx}(\omega) = \sigma_x^2$ it follows that

$$\sigma_y^2 = \frac{\sigma_x^2}{2\pi}\int_{-\pi}^{\pi} |F(\omega)|^2 d\omega.$$

So, the first step to obtain the desired relations is to evaluate the square absolute value of the overall transfer function $F(\omega)$ corresponding to each subband of the filter bank in Fig. 1.

Considering the filters described in Sec. 2 with $p = 1$ and $r = 1$, we easily get the transfer functions of filters at level m as

$$\begin{cases} G_1(\omega) = 2\iota e^{\iota\frac{\omega}{2}}\sin\Big(\dfrac{\omega}{2}\Big), & m = 1, \\ G_m(\omega) = G(2^{m-1}\omega) = 2\iota e^{\iota 2^{m-1}\frac{\omega}{2}}\Big(2^{m-1}\dfrac{\omega}{2}\Big), & m \geq 2, \\ H_m(\omega) = H(2^{m-1}\omega) = \cos^2\Big(2^{m-1}\dfrac{\omega}{2}\Big), & m \geq 1. \end{cases} \tag{3.1}$$

Hence, considering the filter cascade whose output is $d_m(n)$, we can easily derive the square absolute value of overall transfer function G_m^T as

$$\begin{aligned} |G_m^T(\omega)|^2 &= |H_1(\omega)|^2 \cdots |H_{m-1}(\omega)|^2 \cdot |G_m(\omega)|^2 \\ &= 4\sin^2\big(2^{m-1}\tfrac{\omega}{2}\big)\cdot\prod_{k=1}^{m-1}\cos^4\Big(2^{k-1}\frac{\omega}{2}\Big), \quad m \geq 2. \end{aligned} \tag{3.2}$$

and $|G_m^T(\omega)|^2 = 4\sin^2(\frac{\omega}{2})$ for $m = 1$. Analogously, we find

$$|H_m^T(\omega)|^2 = \prod_{k=1}^{m}\cos^4\Big(2^{k-1}\frac{\omega}{2}\Big) \tag{3.3}$$

where $H_m^T(\omega)$ is the transfer function of the filter cascade whose output is $a_m(n)$. Let us state now the first result which will be proved in Sec. 4.

Theorem 3.1. *Given a WSS white additive random process $x(n)$ with variance σ_x^2, let us consider filter bank in Fig.* 1 *with filters $G_m(\omega)$ and $H_m(\omega)$ defined by* (3.1) *and the cascaded transfer function $G_m^T(\omega)$ up to level m given by* (3.2). *Then, the variances of processes $d_m(n)$ and $a_m(n)$, $\sigma_d^2(m)$ and $\sigma_a^2(m)$, respectively, for $m = 1, \ldots, D$, with D number of decomposition levels, are given by*

$$\sigma_d^2(m) = \sigma_x^2\,\frac{2^{2(m-1)}+1}{2^{3(m-1)}}, \quad \sigma_a^2(m) = \sigma_x^2\frac{2^{2m+1}+1}{3\cdot 2^{3m}}. \tag{3.4}$$

In the case $p = 1$, $r = 2$, a common practice is to split the filter $G(\omega)$ into two cascaded gradient filters,[4] $G_I(\omega) = e^{-\frac{\iota\omega}{2}}\big(2\iota\sin\big(\frac{\omega}{2}\big)\big)$ and $G_{II}(\omega) = e^{\frac{\iota\omega}{2}}\big(2\iota\sin\big(\frac{\omega}{2}\big)\big)$,

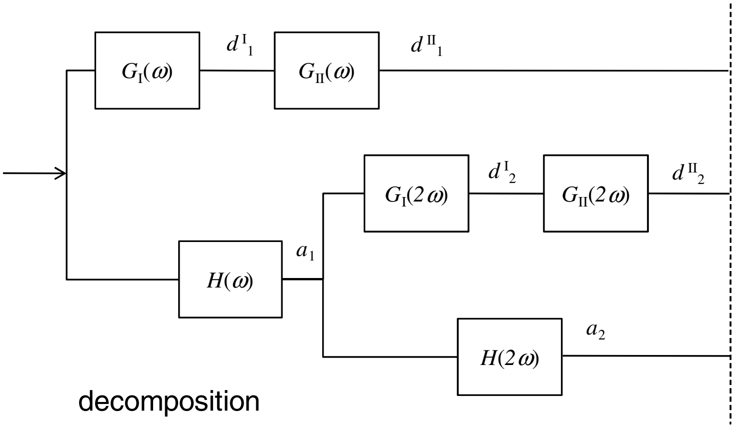

Fig. 3. Splitting of filters G in the case $p = 1$, $r = 2$.

and to apply wavelet thresholding to wavelet coefficients d_m^I at the output of filters G_I (Fig. 3). In fact, performing denoising after the first gradient filter is more efficient since Signal to Noise Ratio (SNR) is higher after G_I than after G_{II}. In contrast, a potential enhancement step is better performed after G_{II}. The noise variance in the coefficients d_m^I, a_m is still given by relations (3.4).

Theorem 3.2 generalizes the above result to the case of two-dimensional WSS white random processes.

Theorem 3.2. *Given a two-dimensional WSS white additive random process* $x(n, q)$, *let us consider filter bank in Fig.* 2, *relations* (3.1) *and* (3.2), *and Theorem* 3.1. *By symmetry of the filter bank in Fig.* 2, *the variance of process* $d_j(m)$, *where* $j = \{v, h\}$ *and* $m = 1, \ldots, D$, *is given by*

$$\sigma^2{}_{d_j}(m) = \sigma_x^2 \frac{(2^{2(m-1)} + 1)(2^{2m-1} + 1)}{3 \cdot 2^{6(m-1)}}. \tag{3.5}$$

The proof of Theorem 3.2 will be given in Sec. 5.

4. Proof of Theorem 3.1

Using (3.2) and recalling that

$$\sigma_y^2 = \frac{\sigma_x^2}{2\pi} \int_{-\pi}^{\pi} |F(\omega)|^2 d\omega,$$

with $\sigma_y^2 = \sigma_d^2(m)$ and $F(\omega) = G_m^T(\omega)$, we get for $\sigma_d^2(m)$

$$\frac{\sigma_x^2}{2\pi} \int_{-\pi}^{\pi} 4\sin^2\left(2^{m-1}\frac{\omega}{2}\right) \cdot \prod_{k=1}^{m-1} \cos^4\left(2^{k-1}\frac{\omega}{2}\right) d\omega, \quad m \geq 2 \tag{4.1}$$

and

$$\frac{\sigma_x^2}{2\pi}\int_{-\pi}^{\pi} 4\sin^2\left(\frac{\omega}{2}\right)\, d\omega = 2\sigma_x^2$$

for $m = 1$. Let us consider now the following identity

$$\prod_{k=1}^{m}\cos^{\alpha}\left(2^{k-1}\frac{\omega}{2}\right) = \left(\frac{\sin(2^{m-1}\omega)}{2^m\sin\left(\frac{\omega}{2}\right)}\right)^{\alpha}, \quad \omega\in\mathbb{R},\ \alpha\in\mathbb{N}. \tag{4.2}$$

The proof can be easily accomplished by induction. So, using (4.2) with $\alpha = 4$, we can rewrite (4.1) as follows

$$\sigma_d^2(m) = \sigma_x^2\,\frac{1}{2\pi}\int_{-\pi}^{\pi} 4\sin^2\left(2^{m-1}\frac{\omega}{2}\right)\cdot P_m(\omega)d\omega, \tag{4.3}$$

where

$$P_m(\omega) = \begin{cases}\left(\dfrac{\sin(2^{m-2}\omega)}{2^{m-1}\sin\left(\frac{\omega}{2}\right)}\right)^4, & m\geq 2,\\ 1, & m = 1.\end{cases}$$

To evaluate the last integral, some results from analytic function theory will be applied. When dealing with integral of the form $I = \int_0^{2\pi}R(\cos(x),\sin(x))dx$, where R is a generic rational function, the solution can be accomplished by reducing it to the integral of an analytic function of a complex variable on a closed curve. Introducing the complex variable $z = e^{\iota x}$, we have $\cos(x) = \frac{z+z^{-1}}{2}$ and $\sin(x) = \frac{z-z^{-1}}{2\iota}$. So, the generic integral is transformed into the following $I = \frac{1}{\iota}\int_{|z|=1}R(\frac{z+z^{-1}}{2},\frac{z-z^{-1}}{2\iota})\frac{dz}{z}$. Using that $I = 2\pi\sum_{k=1}^{M}\mathrm{Res}[\tilde{R}(z),z_k]$, where $\tilde{R} = \frac{1}{z}R(\frac{z+z^{-1}}{2},\frac{z-z^{-1}}{2\iota})$ and $\mathrm{Res}[\tilde{R}(z),z_k]$ denotes the residue of $\tilde{R}(z)$ in z_k, we finally get

$$I = 2\pi\sum_{k=1}^{M}\frac{1}{(\alpha_k-1)!}\lim_{z\to z_k}\frac{d^{\alpha_k-1}}{dz^{\alpha_k-1}}[(z-z_k)^{\alpha_k}\tilde{R}(z)],$$

where α_k is the order of the pole z_k, $k = 1,\ldots,M$. Let us apply the above results to (4.3) in the case $m\geq 2$.

By setting $\frac{\omega}{2} = x$, from the symmetry and the π-periodicity of the integrand, it follows

$$\sigma_d^2(m) = \frac{\sigma_x^2}{2\pi}\int_0^{2\pi} 4\sin^2(2^{m-1}x)\left(\frac{\sin(2^{m-1}x)}{2^{m-1}\sin(x)}\right)^4 dx.$$

Using Euler's relations and setting $s = 2^{m-1}$, we get

$$\sigma_d^2(m) = \frac{\sigma_x^2}{2\pi}\int_0^{2\pi}\frac{4}{s^4}\left(\frac{e^{\iota sx}-e^{-\iota sx}}{2\iota}\right)^6\left(\frac{2\iota}{e^{\iota x}-e^{-\iota x}}\right)^4 dx.$$

By setting now $z = e^{\iota x}$, we get

$$\begin{aligned}
\sigma_d^2(m) &= \frac{\sigma_x^2}{2\pi\iota}\int_{\Gamma_1^+} \frac{4}{s^4\, z}\left(\frac{z^s - z^{-s}}{2\iota}\right)^6 \left(\frac{2\iota}{z - z^{-1}}\right)^4 dz \\
&= \frac{\sigma_x^2}{2\pi\iota}\int_{\Gamma_1^+} \frac{4}{s^4\, z}\left(\frac{z^{2s} - 1}{2\iota z^s}\right)^6 \left(\frac{2\iota z}{z^2 - 1}\right)^4 dz \\
&= \frac{-\sigma_x^2}{2\pi\iota}\int_{\Gamma_1^+} \frac{1}{s^4}\left(\frac{z^{2s} - 1}{z^2 - 1}\right)^4 \frac{(z^{2s}-1)^2}{z^{6s-3}}\, dz,
\end{aligned}$$

where Γ_1^+ denotes the circle $\{|z| = 1\}$ positively oriented. Since $\left(\frac{z^{2s}-1}{z^2-1}\right)^4 = \left(\sum_{k=0}^{s-1} z^{2k}\right)^4$, we get

$$\sigma_d^2(m) = \frac{-\sigma_x^2}{2\pi\iota}\int_{\Gamma_1^+} \frac{1}{s^4}\left(\sum_{k=0}^{s-1} z^{2k}\right)^4 \frac{1 - 2z^{2s} + z^{4s}}{z^{6s-3}} dz$$

and thus the only singularity is in $z = 0$, with order $\alpha_0 = 6s - 3$. Using the above results, we get

$$\sigma_d^2(m) = \frac{-\sigma_x^2}{s^4(6s-4)!}\cdot \lim_{z\to 0} \frac{d^{6s-4}}{dz^{6s-4}} f(z)$$

where

$$f(z) = \left(\sum_{k=0}^{s-1} z^{2k}\right)^4 \cdot (1 - 2z^{2s} + z^{4s}).$$

Note that in order to determine $\sigma_d^2(m)$ it is sufficient to evaluate the multiplicative coefficient of the term of order $6s - 4$ in the function $f(z)$. Terms of order $6s - 4$ in $f(z)$ correspond to the terms of order $6s - 4$, $4s - 4$, and $2s - 4$ in $\left(\sum_{k=0}^{s-1} z^{2k}\right)^4$. Let us evaluate them one by one. In order to compute the term of order $6s - 4$, consider the scheme in Fig. 4 where the two rows correspond to $\left(\sum_{k=0}^{s-1} z^{2k}\right)^2$. The $(s - 1)$ arrows point out the only products of order $6s - 4$, whose sum can be

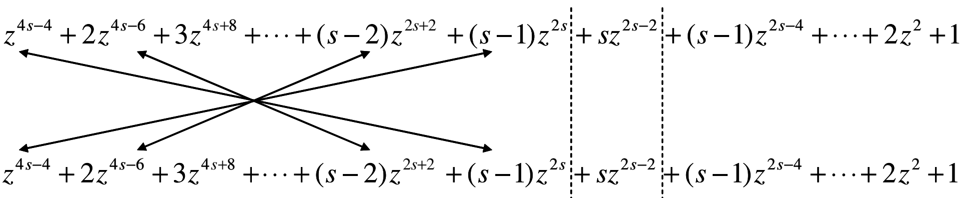

Fig. 4. Evaluation of the term of order $6s - 4$.

written as

$$
\begin{aligned}
&z^{4s-4}z^{2s}\cdot(s-1)+2\cdot z^{4s-6}z^{2s+2}\cdot(s-2)+\cdots+(s-1)\cdot z^{2s}z^{4s-4}\\
&\quad = z^{6s-4}\sum_{k=1}^{s-1}k(s-k) = z^{6s-4}\left(s\sum_{k=1}^{s-1}k-\sum_{k=1}^{s-1}k^2\right).
\end{aligned}
$$

Recalling now that

$$
\sum_{k=1}^{s-1}k=\frac{s(s-1)}{2},\quad \sum_{k=1}^{s-1}k^2=\frac{s(s-1)(2s-1)}{6},
$$

we finally get that the sum of the $(s-1)$ products is equal to

$$
z^{6s-4}\left(s\frac{s(s-1)}{2}-\frac{s(s-1)(2s-1)}{6}\right). \tag{4.4}
$$

By symmetry, it follows that the term of order $2s-4$ is the same. The terms of order $4s-4$ can be obtained as shown in Fig. 5. The arrows identify $2s-1$ products whose sum can be written as

$$
\begin{aligned}
&z^{4s-4}+2\cdot z^{4s-6}z^2\cdot 2+\cdots+(s-1)z^{2s}z^{2s-4}\cdot(s-1)\\
&\qquad + s\cdot z^{2s-2}z^{2s-2}\cdot s+\cdots+2\cdot z^2z^{4s-6}\cdot 2+z^{4s-4}\\
&\quad = z^{4s-4}\left(\left(\sum_{k=1}^{s-1}k^2\right)+s^2+\left(\sum_{k=1}^{s-1}k^2\right)\right)\\
&\quad = z^{4s-4}\left(s^2+2\sum_{k=1}^{s-1}k^2\right)\\
&\quad = z^{4s-4}\left(2\left(\frac{s(s-1)(2s-1)}{6}\right)+s^2\right).
\end{aligned} \tag{4.5}
$$

Since the term of order $4s-4$ must be multiplied by -2, we finally get that the global term of order $6s-4$ in $f(z)$ is given by (4.4) multiplied by 2 plus (4.5)

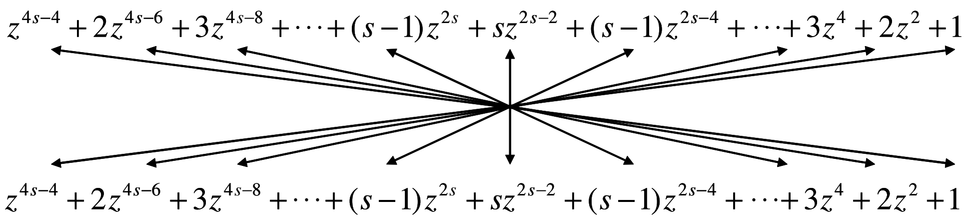

Fig. 5. Evaluation of the term of order $4s-4$.

multiplied by -2, that is $z^{6s-4}(-s(s^2+1))$. Consequently, we obtain

$$\sigma_d^2(m) = \frac{-\sigma_x^2}{s^4} \cdot (-s(s^2+1)) = \sigma_x^2 \frac{s^2+1}{s^3}.$$

Recalling now that $s = 2^{m-1}$, we get the left part of (3.4). If $m = 1$ the result follows immediately by (4.1). Using (4.2), we obtain

$$\sigma_a^2(m) = \frac{\sigma_x^2}{2\pi} \int_{-\pi}^{\pi} \left(\frac{\sin(2^{m-1}\omega)}{2^m \sin\left(\frac{\omega}{2}\right)} \right)^4 d\omega$$

Exploiting symmetry and periodicity properties of functions involved and substituting $\frac{\omega}{2} = x$, we get

$$\sigma_a^2(m) = \sigma_x^2 \frac{1}{2\pi} \int_0^{2\pi} \left(\frac{\sin(2^m x)}{2^m \sin(x)} \right)^4 dx.$$

Setting now $s = 2^m$ and $z = e^{\iota x}$ and arguing as in the evaluation of $\sigma_d^2(m)$, it also follows

$$\begin{aligned} \sigma_a^2(m) &= \sigma_x^2 \frac{1}{2\pi\iota} \int_{\Gamma_1^+} \left(\frac{z^s - z^{-s}}{z - z^{-1}} \right)^4 \frac{1}{z\, s^4}\, dz \\ &= \sigma_x^2 \frac{1}{2\pi\iota} \int_{\Gamma_1^+} \left(\frac{z^{2s} - 1}{z^2 - 1} \right)^4 \frac{1}{z^{4s-3}\, s^4}\, dz \\ &= \lim_{z \to 0} \sigma_x^2 \frac{1}{s^4\,(4s-4)!} \frac{d^{4s-4}}{dz^{4s-4}} \left[\left(\sum_{k=0}^{s-1} z^{2k} \right)^4 \right]. \end{aligned}$$

Now, considering again Fig. 5, the term of order $4s-4$ can be written as

$$z^{4s-4} \left(2 \sum_{k=0}^{s-1} k^2 + s^2 \right) = z^{4s-4} \left(\frac{s(s-1)(2s-1)}{3} + s^2 \right) = z^{4s-4} \frac{2s^3 + s}{3}$$

and hence we finally obtain

$$\sigma_a^2(m) = \sigma_x^2 \frac{2s^3 + s}{3s^4} = \sigma_x^2 \frac{2^{2m+1} + 1}{3 \cdot 2^{3m}}, \quad m = 1, \ldots, D.$$

5. Proof of Theorem 3.2

In order to prove relation (3.5), observe that at level $m-1$ filter h has to be applied twice (firstly, on the rows and then on the columns of the input signal) before applying filter g at level m. Then, owing to separability of filters, the variance of vertical detail coefficients at level m can be expressed by

$$\sigma_{d_v}^2(m) = \frac{\sigma_x^2}{(2\pi)^2} \int_{-\pi}^{\pi} \left(\prod_{k=1}^{m-1} |H_k(\omega_v)|^2 \right) |G_m(\omega_v)|^2\, d\omega_v \cdot \int_{-\pi}^{\pi} \prod_{j=1}^{m-1} |H_j(\omega_h)|^2\, d\omega_h,$$

for $m \geq 2$ (for $m = 1$ it is easily get by Sec. 2). So, applying right part of (3.4) at level $m - 1$, we obtain the multiplicative coefficient

$$r(m) = \frac{2^{2(m-1)+1} + 1}{3 \cdot 2^{3(m-1)}} = \frac{2^{2m-1} + 1}{3 \cdot 2^{3(m-1)}}$$

that concerns second integral in the last expression. Then, using the left part of (3.4) at level m to compute the first integral and multiplying by $r(m)$ we finally get the thesis. By symmetry, the same expression holds for $\sigma^2_{d_h}(m)$. In a similar fashion, one can derive the analogous expression for $\sigma^2_a(m)$.

6. Conclusion

In this paper, we have considered a particular class of DDWT based on spline functions and we have provided a direct relation between noise power in original signal and noise power in each subband of wavelet decomposition, under the assumption of a WSS white additive random noise. This relationship is of fundamental importance for denoising, since in most of the threshold-selection methods the knowledge of the subband variance is required.

The paper does not address the case of signal dependent noise such as quantum noise encountered in CCD-based acquisition devices or scan film radiography. In this case, homoscedasticity cannot be assumed and relations used in Sec. 3 have to be modified.

References

1. S. G. Chang, B. Yu and M. Vetterli, Adaptive wavelet thresholding for image denoising and compression, *IEEE Trans. Image Process.* **9**(9) (2000) 1532–1546.
2. D. Donoho, Denoising by soft-thresholding, *IEEE Trans. Inform. Theory* **41**(3) (1995) 613–627.
3. D. L. Donoho and I. M. Johnstone, Ideal spatial adaptation by wavelet shrinkage, *Biometrika* **81** (1994) 425–455.
4. J. Fan and A. Laine, Contrast enhancement by multiscale and nonlinear operators, in *Wavelets in Medicine and Biology*, eds. A. Aldroubi and M. A. Unser (CRC Press, 1996), pp. 163–192.
5. J. E. Fowler, The redundant discrete wavelet transform and additive noise, *IEEE Signal Process. Lett.* **12**(9) (2005) 629–632.
6. P. Gravel, B. Gilles and J. A. De Guise, A method for modeling noise in medical images, *IEEE Trans. Med. Imag.* **23**(10) (2004) 1221–1232.
7. M. Holschneider, R. Kronland-Martinet, J. Morlet and P. Tchaminchian, *Wavelets, Time-Frequecy Methods and Phase Space* (Springer-Verlag, Berlin, Germany, 1989).
8. A. Khare and U. S. Tiwary, Soft-thresholding for denoising of medical images. A multiresolution approach, *Int. J. Wavelets Multiresolut. Inf. Process.* **3**(4) (2005) 477–496.
9. I. Koren and A. Laine, A discrete dyadic wavelet transform for multidimensional feature analysis, in *Time-Frequency and Wavelet Transform in Biomedical Engineering*, ed. M. Akay (IEEE Press, USA, 1997), pp. 425–449.
10. S. Mallat, *A Wavelet Tour of Signal Processing* (Academic Press, San Diego, USA, 1998).

11. S. Mallat and S. Zhong, Characterization of signals from multiscale edges, *IEEE Trans. Pattern Anal. Mach. Intell.* **14**(7) (1992) 710–732.
12. A. Mencattini, M. Salmeri, S. Bertazzoni and A. Salsano, Noise variance estimation in digital images using iterative fuzzy procedure, *WSEAS Trans. Systems* **4**(2) (2003) 1048–1056.
13. A. Mencattini, M. Salmeri, R. Lojacono and M. Arnò, Noise estimation in mammographic images for adaptive denoising, in *EFOMP European Conf. Medical Physics*, Castelvecchio Pascoli, Italy (September, 2007), pp 1–2.
14. A. Mencattini, M. Salmeri, R. Lojacono, M. Frigerio and F. Caselli, Mammographic images enhancement and denoising for breast cancer detection using dyadic wavelet processing, *IEEE Trans. Instrum. Meas.* **57**(7) (2008) 1422–1430.
15. M. Rank, M. Lendl and R. Unbehauen, Estimation of image noise variance, *IEE Proc. Vis. Image Signal Process.* **146** (1999) 80–84.
16. T. A. Türüki, M. Hussain, K. Niijima and S. Takano, The dyadic lifting schemes and the denoising of digital images, *Int. J. Wavelets Multiresolut. Inf. Process.* **6**(3) (2008) 331–351.
17. M. Unser, A. F. Laine and A. Aldroubi, Special issue on wavelets on medical imaging, *IEEE Trans. Med. Imag.* **22**(3) (2003) 285–288.
18. X. Yang, X. Zhang and Z. Zhu, Frame-based image denoising using hidden Markov model. *Int. J. Wavelets Multiresolut. Inf. Process.* **6**(3) (2008) 419–432.
19. C. Zhang, X. Wang, H. Zhang and C. Duanmu, An anti-noise algorithm for enhancing global and local contrast for infrared image, *Int. J. Wavelets Multiresolut. Inf. Process.* **5**(1) (2007) 101–112.